

ADVANCED CHARACTERIZATION OF MICROSTRUCTURES IN ULTRA HIGH STRENGTH DUAL PHASE STEEL

Jason Andring¹, Cyrus Eason¹, and Dr. Anthony DeArdo^{1,2}

¹Basic Metals Processing Research Institute

Department of Mechanical Engineering and Materials Science, University of Pittsburgh;

636 Benedum Hall, 3700 O'Hara Street, Pittsburgh PA 15261

²Centre for Advanced Steels Research, Materials Engineering Laboratory

Department of Mechanical Engineering, P.O Box 4200

FI-90014 University of Oulu, Oulu, Finland

Keywords: Dual phase steel, fractal analysis, nanohardness of individual phases, hole expansion ratio

Abstract

The hardnesses of ferrite and martensite were measured using nanoindentation of each phase. It was found that the sheared hole expansion ratio (HER) is directly related to the ratio of the hardnesses of the hard (martensite) and soft (ferrite) phases. The increase in hardness of both phases occurred during testing, i.e. hole punching and expansion. In the case of the ferrite this increase is due to second stage work hardening attributed to the co-deformation of ferrite and martensite. A strong positive linear correlation exists between the hardness difference between ferrite and martensite of the undeformed plate and UTS where larger differences lead to higher UTS but low HER. Fractal analysis has also been investigated to characterize the ferrite/martensite interface where higher fractal dimensions (rougher boundaries) of more complex microstructures lead to a reduction in HER.

Introduction

Dual phase (DP) steels are widely used for automotive applications due to certain advantages these materials have over other conventional steels such as permitting lower weight and production costs, and improved crash resistance and fatigue strength. Strengthening of the composite is achieved through optimizing the volume fraction of martensite and by strengthening the ferrite in the usual way, i.e.: solid-solution hardening, precipitation hardening, and grain refinement [1]. Variations in alloying and processing parameters such as coiling temperature, cold reduction, and tempering can lead to large variations in the desired microstructures and final properties of the DP steel. Different intercritical annealing temperatures will lead to differences in martensite volume fraction, composition, strength, and grain size when quenched [2].

The stretch flanging capabilities of sheet metal is generally measured through the use of hole expansion tests. Hole expansion tests quantify the hole flangeability into the hole expansion ratio (HER) which is the percent difference between the initial and final hole diameters [3]. However, as shown by Xu, *et al.* [4], the hole formation process greatly effects the maximum HER obtainable. Cutting methods such as laser cutting, and electrical discharge machining produce high HERs. Processes, such as hole punching, leave substantial amounts of surface damage (microcrack formation), and macroscopic unevenness which greatly reduce the HER [5]. The punched hole surface can be machined and smoothed to increase the HER [6], but may not be economically

feasible. Thus, fractures of sheared hole edges is more sensitive to local fractures and are more dependent on microstructural features to resist local cracking [7]. Microstructural properties such as the phase hardness, morphology, grain size, and hard phase volume fraction can be seen to improve HER [8]. Not only does the hard phase provide dispersion strengthening, but also aids in reducing plastic strain within the ferrite during expansion and allows for higher HER based off finite element analysis [9]. Other studies show that the HER can depend on macroscopic properties such as yield stress, ultimate tensile stress, uniform elongation, average normal anisotropy, strain rate, and both strain hardening rate and exponents [10].

One of the most common microstructural properties to directly affect the HER is thought to be the hardness difference between the phases. The hardness can be measured by utilizing a number of different methods, however, nanoindentation provides the most accurate way to measure the very fine grains of DP steels. Taylor, *et al.* [11], showed that with increasing constituent hardness decreased HER but also increases yield strength. The morphology of martensite islands also impacts the HER and other mechanical properties of DP steels. It was found that a uniform distribution of fine and fibrous martensite islands leads to higher strength and ductility [11,12]. The morphology also affects the work hardening of DP steel where different stages of deformation occurs in the ferrite and martensite [13]. Hornbogen [14], introduced using fractal analysis as a way to systematically characterize the grain boundaries and complexity of microstructures. This can be done through numerous methods, though box counting is one of the simplest. The fractal dimension D_b is calculated as the slope of the plot $\ln N_i$ against $\ln \epsilon_i^{-1}$.

$$D_b = \frac{\ln N_i}{\ln \epsilon_i^{-1}} \quad (1)$$

Where N_i is the number of boxes that intersect the ferrite/martensite interface at the box scales ϵ_i . The fractal dimension is then the measure of interface roughness or complexity [15,16]. As a result, D_b could be used to characterize observed microstructural features.

Procedure

The steels in this study all had the chemical composition in *Table 1*.

Table 1: Chemical composition of steel samples [17].

Chemical Composition (wt%)												
Elements	C	Mn	P	S	Si	Cr	Mo	V	Ti	Al	N	Nb
	0.15	1.8	0.01	0.003	0.4	0.5	0.3	0.06	0.005	0.025	0.006	0.005

Processing

Metal sheets were produced through a series of thermomechanical processing by varying several processing parameters such as hot band coiling temperature (CT), cold reduction (CR), intercritical annealing temperature (IAT), and isothermal holding time (IHT) in the zinc pot held at 460 °C. The thermomechanical processing steps are schematically shown in *Figure 2*. Laboratory slabs were hot rolled at 1250 °C from an initial thickness of 25 mm to 5 mm after 5 passes (27.5% reduction with each pass) and coiled at 500 or 650 °C, with slow cooling to room temperature. The surfaces were ground, reducing the thickness to 3 mm, then cold rolled to either

1.24 or 0.85 mm, representing cold reductions of 58% or 72%, respectively. Two different annealing paths were used: standard galvanizing, and supercool processing [18,19]

Standard galvanizing (labeled F1) involved annealing the cold rolled sheets at either 750 or 770 °C for 60 s, then cooling at 15 °C/s to the zinc pot temperature of 460 °C and held there for 15 or 30 s, followed by cooling to room temperature at 10 °C/s. The Supercool process (labeled G1) involved annealing at either 750 or 770 °C for 60 s, cooling to 200 °C at 15 °C/s and held for 20 s. Then the temperature was increased to the zinc pot temperature and held for either 15 or 30 s, after which it was cooled to room temperature at 10 °C/s. The processing of each sample is summarized in *Table 1* [17].

Table 1: Processing parameters and tensile test properties for steel samples [17].

Sample	Processing				Mechanical Properties					
	CT (°C)	CR (%)	IAT (°C)	IHT (s)	UTS (MPa)	HER (%)	RA (%)	TE (%)	n1	n2
5M8KF1	500	58	770	30	1211	13.65	25.72	15.54	0.240	0.100
6M8JF1	650	58	770	15	1257	7.80	23.44	14.59	0.640	0.108
6N7KF1	650	72	750	30	1266	14.21	20.64	15.6	0.340	0.130
5M8JG1	500	58	770	15	1054	35.13	33.77	18.91	0.807	0.097
6M8JG1	650	58	770	15	1085	35.65	34.67	21.23	0.872	0.097
6M8KG1	650	58	770	30	1083	25.21	37.75	16.63	0.200	0.090

Hole Expansion Ratio Testing

Holes with a diameter of 10 mm were punched in the center of 80 x 100 mm steel sheets. The hole was then expanded by a 60° conical punch at 0.3 mm/s and stopped at the onset of a crack which extended through the full sheet thickness.

Nanoindentation

Areas that contained a large volume fraction of ferrite were marked with a triangular shaped pattern with Vickers indents at 300 gf using a leco LM800 Microhardness Tester. Along each sample several areas were marked where the strain varied from the hole expansion tests. An area of no additional strain (Position 1), low additional strain (Position 2), and a high additional strain (Position 3) area as close as possible to the shear zone around the hole. Nanoindentation was used to measure the hardness of ferrite and martensite within each position on a completely polished surface. Indents were carried on a TriboIndenter Hysitron in a 5x5 grid and spaced 4 μm at a maximum load of 2000 μN. Nanoindents were then viewed at 6500x magnification using a FEI Apreo Scanning Electron Microscope.

Fractal Analysis

ImageJ with the FracLac plugin was used to calculate the fractal dimension using the box count method. SEM images were processed into binary images where the ferrite/martensite interphases could be obtained with the “find edges” function. For each image, the fractal dimension was measured with 20 grids starting at random positions and box scaling from 0.7122 to 0.0016 with 100 grid iterations.

Results

Images obtained through the SEM are displayed for 6N7KF1 (CT = 650 °C, CR = 72%, IAT = 750 °C, IHT = 30 s) in *Figure 1*. Accepted indents that were either fully in the ferrite (red) or martensite (blue) were used to calculate the average nanoindentation hardness (NIH) within each area. Across the ribbon, the ferrite hardness changes drastically between the no and high strain areas. Although slight differences within the martensite hardness is observed. This indicates that HER is mainly dependent on the martensite phase. Due to essentially no retained austenite in these steels, the hardness is seen to increase according to second stage strain hardening with the co-deformation of both phases. The hardness of the no strain areas is summarized in *Table 2*.

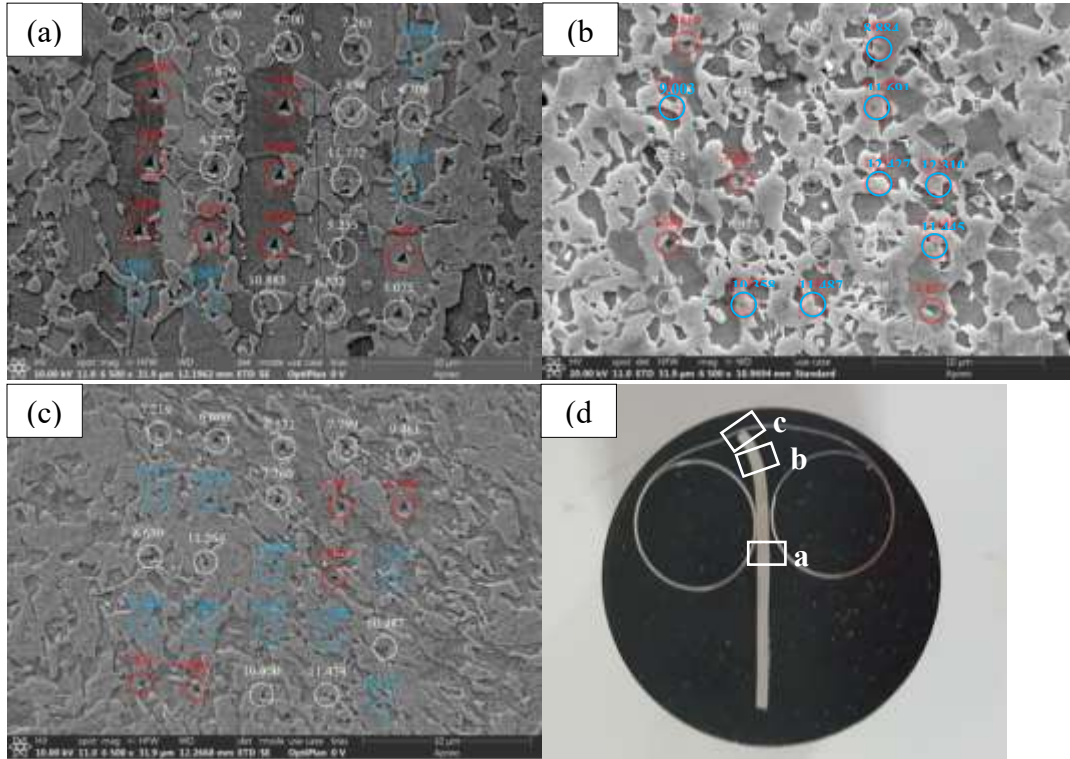


Figure 1: Standard galvanized sample 6N7KF1 (CT = 650 °C, CR = 72%, IAT = 750 °C, IHT = 30 s). Indentations and corresponding hardness values for (a) no strain, (b) low strain and (c) high strain areas. (d) Shows the SEM orientation.

Table 2: Measured ferrite and martensite hardness, and fractal dimensions of the no strain areas.

	NIH α	NIH α'	Δ NIH	α/α'	D_b
Designation	(GPa)	(GPa)	(GPa)		
5M8KF1	4.28	10.31	6.03	0.42	1.6792
6M8JF1	4.23	9.75	5.51	0.43	1.6497
6N7KF1	3.94	10.03	6.08	0.39	1.5894
5M8JG1	4.80	7.87	3.07	0.61	1.5400
6M8JG1	4.73	6.25	1.51	0.76	1.5897

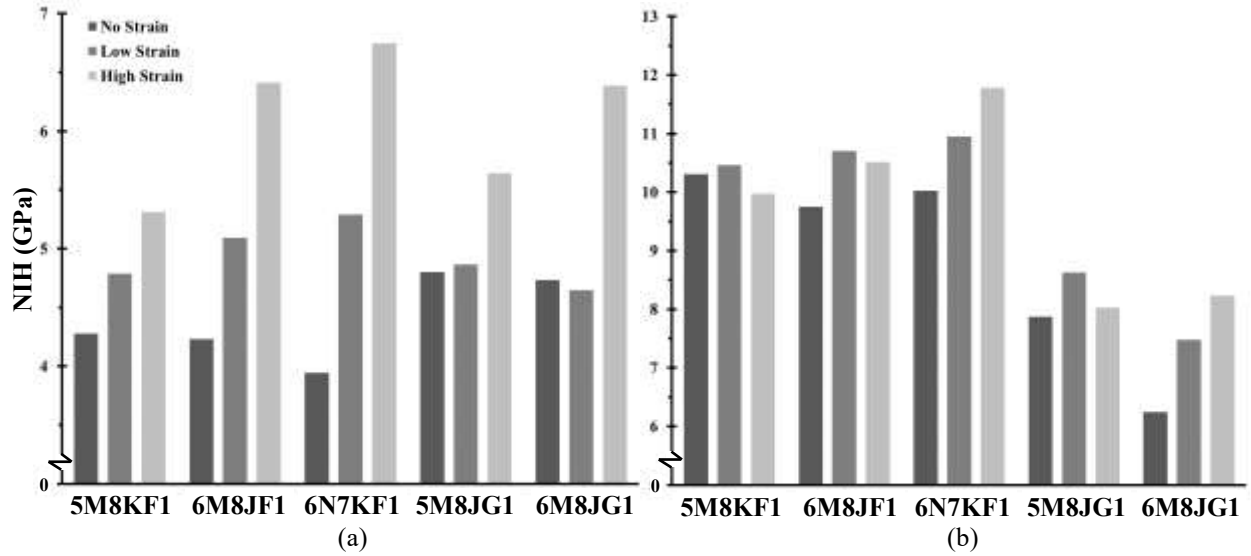


Figure 2: NIH across the no, low, and high strain areas for (a) ferrite and (b) martensite.

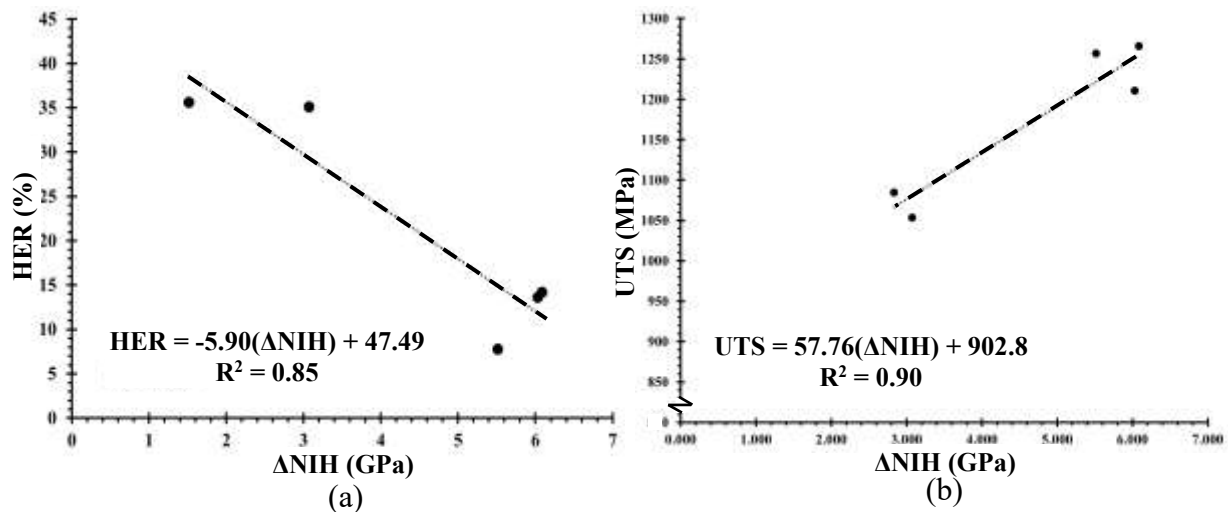


Figure 3: The NIH difference, ΔNIH , between ferrite and martensite and the relationship to the (a) measured HER and (b) UTS.

The NIH across all positions is summarized in Figure 2. The supercooled samples (G1) show higher ferrite hardness in the low strain areas than the standard galvanized (F1) samples. This may be due to more carbon in solid solution with more martensite tempering. Although both supercooled samples were both held isothermally at 15 s and show similar hardness. However, martensite hardness is drastically higher in the standard galvanized samples. The difference in NIH between the ferrite and martensite was then plotted against mechanical properties such as HER and UTS, shown in Figure 3 (a) and (b), which shows strong negative and positive linear correlations, respectively. As a result, the HER and UTS can be approximately predicted from the hardness difference using eq. (2) and (3),

$$\text{HER} = -5.90(\Delta\text{NIH}) + 47.49 \quad (2)$$

And

$$UTS = 57.76(\Delta NIH) + 902.8 \quad (3)$$

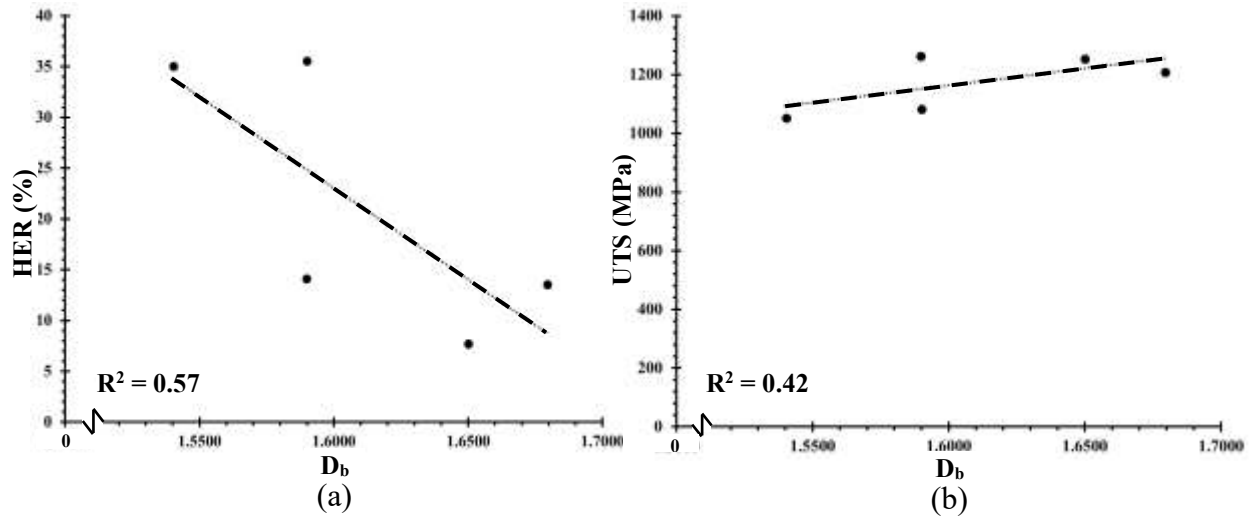


Figure 4: The fractal dimension plotted against the (a) HER and (b) UTS.

The measured fractal dimensions based off the SEM images is also summarized in *Table 2*. Weak negative and positive linear correlations are seen between the HER and UTS respectively, shown in *Figure 4(a)* and *(b)*. This leads to the assumption that with increasing ferrite/martensite interface roughness or complexity creates a negative impact on the HER, but a positive impact on the UTS.

Discussion

It was seen that the dual phase steels with ferrite and martensite microconstituents and relatively high volume fractions of martensite (50 – 70%) show deformation that is attributed to both ferrite and martensite phases. As a result, mechanical properties such as the total elongation, the reduction in area, and the ultimate tensile strength experience strong correlations with the HER. Other properties which depend on the deformation of ferrite, such as the yield strength, provide no correlation with the HER. The hardness of the martensite stayed relatively constant around 10.5 GPa regardless of the strain of the microstructure, which may suggest that the HER is mainly controlled by the hard phase with high volume fractions. However, 6N7KF1 (CT = 650 °C, CR = 72%, IAT = 750 °C, IHT = 30 s) showed the highest HER despite being cold rolled 72% as opposed to 58%. This sample, which exhibited higher deformation of the martensite islands than the other two standard galvanized samples, was seen to have the higher change in martensite hardness.

The fractal dimension may provide more insight in how the morphology of the ferrite/martensite interface affects the HER. Higher fractal dimensions are attributed to a rougher interface between ferrite and martensite, which may be detrimental to the HER. Further investigations need to be carried out on a wider selection of DP steels to fully explore the suggested relationship between the mechanical properties and the fractal dimension of the steel. Better insight may be gleaned from applying the box count method to the whole of the sample, instead of only the no strain area, which showed a weak correlation between D_b and the other properties. Also, other methods to measure the fractal dimension, such as the yard stick method

or the perimeter-area relationship used by Streitenberger, et al. [18], may be useful in analyzing the ferrite/martensite interface.

Conclusion

Dual phase steels are dependent on many different microstructural factors. These include the fracture toughness, grain size, volume fraction and morphology of the hard phase, as well as the microconstituent hardnesses, which produce a wide range of observed properties. Better ability to characterize the microstructural features of the steel may provide insight enough to produce stronger and more ductile steels. Through the use of nanoindentation, the hardness differentials between both phases can be determined and used as a strong indicator of the steel's mechanical properties, such as the reduction of area, ultimate tensile strength, and total elongation. Larger differences in the hardnesses of the phases drastically reduce the ductility of the steel. Fractal analysis may also be an important tool in quantifying the microstructure, and in describing its irregularity. Greater fractal dimensions are attributed to microstructures with rougher grain boundaries, which negatively influence the ductility of the steel.

References

- [1] S.L. Semiatin, 52.1 Classification of HSS and AHSS, ASM Handbook, Vol. 14B - Metalwork. Sheet Form. (n.d.). <https://app.knovel.com/hotlink/khtml/id:kt008I27V1/asm-handbook-volume-14b/classification-hss-ahss>.
- [2] G. Krauss, *Steels: Processing, Structure, and Performance*, 2nd ed., ASM International, 2015.
- [3] X. Chen, H. Jiang, Z. Cui, C. Lian, C. Lu, Hole Expansion Characteristics of Ultra High Strength Steels, *Procedia Eng.* 81 (2014) 718–723. doi:<https://doi.org/10.1016/j.proeng.2014.10.066>.
- [4] L. Xu, F. Barlat, M. G. Lee, K. S. Choi, X. Sun, Hole expansion of dual phase steels, *WIT Trans. Built Environ.* 124 (2012) 75–83.
- [5] K. Mori, Y. Abe, Y. Suzui, Improvement of Stretch Flangeability of Ultra High Strength Steel sheet by Smoothing of Sheared edge, *J. Mater. Process. Technol.* 210 (2010).
- [6] K. Mori, Y. Abe, Y. Ikeda, Improvement of Formability for Expansion of Punched Hole of Ultra-High Strength Steel Sheets by Smoothing of Sheared edge, *Steel Res. Int.* (2011).
- [7] F. Hisker, R. Thiessen, T. Heller, Influence of Microstructure on Damage in Advanced High Strength Steels, in: *THERMEC 2011*, Trans Tech Publications, 2012: pp. 925–930. doi:10.4028/www.scientific.net/MSF.706-709.925.
- [8] V. Nallasivam, S. Misra, Effect of microstructure on the hole expansion properties of advanced high-strength steels, (2016).
- [9] J.H. Kim, M.G. Lee, D. Kim, D.K. Matlock, R.H. Wagoner, Hole-expansion formability of dual-phase steels using representative volume element approach with boundary-smoothing technique, *Mater. Sci. Eng. A.* 527 (2010) 7353–7363. doi:<https://doi.org/10.1016/j.msea.2010.07.099>.
- [10] J.H. Kim, Y.J. Kwon, T. Lee, K.-A. Lee, H.S. Kim, C.S. Lee, Prediction of hole expansion ratio for various steel sheets based on uniaxial tensile properties, *Met. Mater. Int.* 24 (2018) 187–194. doi:10.1007/s12540-017-7288-2.
- [11] M.D. Taylor, K.S. Choi, X. Sun, D.K. Matlock, C.E. Packard, L. Xu, F. Barlat, Correlations between nanoindentation hardness and macroscopic mechanical properties in DP980 steels, *Mater. Sci. Eng. A.* 597 (2014).

- [12] F. Zhang, A. Ruimi, P.C. Wo, D.P. Field, Morphology and distribution of martensite in dual phase (DP980) steel and its relation to the multiscale mechanical behavior, *Mater. Sci. Eng. A.* 659 (2016) 93–103. doi:<https://doi.org/10.1016/j.msea.2016.02.048>.
- [13] D. Das, P.P. Chattopadhyay, Influence of martensite morphology on the work-hardening behavior of high strength ferrite--martensite dual-phase steel, *J. Mater. Sci.* 44 (2009) 2957–2965. doi:10.1007/s10853-009-3392-0.
- [14] E. Hornbogen, A systematic description of microstructure, *J. Mater. Sci.* 21 (1986) 3737–3747. doi:10.1007/BF02431607.
- [15] Y. Kang, H.K.D.H. Bhadeshia, Roughness of Bainite, *Mater. Sci. Technol.* 22 (2006).
- [16] H. Su, Z. Yan, J.T. Stanley, Fractal analyses of microstructure and properties of HSLA steels, *J. Mater. Sci. Lett.* 14 (1995) 1436–1439. doi:10.1007/BF00462207.
- [17] Y. Wu, PROCESSING, MICROSTRUCTURES AND PROPERTIES OF ULTRA-HIGH STRENGTH, LOW CARBON AND V-BEARING DUAL-PHASE STEELS PRODUCED ON CONTINUOUS GALVANIZING LINES, University of Pittsburgh, 2017.
- [18] Y. Gong, M. Hua, J. Uusitalo, A.J. DeArdo, Improving the Sheared-Edge Formability of High-Strength Dual-Phase Steel, in: AIST (Ed.), AISTech 2016 Proc., 2016.
- [19] Y. Gong, M. Hua, J. Uusitalo, A.J. DeArdo, Effects of Thermomechanical Processing and Vanadium Additions on Microstructures and Properties of High Strength Dual Phase Steels Processed with Continuous Galvanizing Line Simulations, in: Contrib. Pap. from Mater. Sci. Technol. 2015, MS&T, 2015.